

COVER PAGE

Document downloaded by @DAEL

Sun Nov 8 06:32:02 2026
For personal use

When automatic English translation is provided, only the original document is authentic.
The EAA cannot be held responsible of any translation error

Bibliographical reference

A Dome Shaped PVDF Loudspeaker Model, B. Gazengel, P. Hamery, P. Lotton and A. Ritty, Acta Acustica **vol. 97** (Number 5), 2011, pp. 800-808

DOI
https://doi.org/10.3813/AAA.918460

Acta Acustica united with Acustica
Vol. 97 (2011) 800 – 808

DOI 10.3813/AAA.918460

A Dome Shaped PVDF Loudspeaker Model

B. Gazengel[1)], P. Hamery[2)], P. Lotton[1)], A. Ritty[2)]

[1)] Laboratoire d'Acoustique de l'Université du Maine, UMR CNRS 6613, Université du Maine, Avenue Olivier Messiaen, 72085 Le Mans Cedex 9, France. [bruno.gazengel, pierrick.lotton]@univ-lemans.fr

[2)] Institut Franco-Allemand de Recherches de Saint Louis (ISL), 5, rue Général Cassagnou 68300 Saint-Louis, France. hamery@isl.tm.fr

Summary

An analytical model is developed that describes the behavior of a dome-shaped piezoelectric loudspeaker. The loudspeaker consists of a PVDF circular membrane coupled with a rear cylindrical cavity. The dome shape is obtained by means of a static differential pressure held between the two faces of the membrane. The theoretical description of the transducer's behavior is conducted in two steps. In the first step, the static behavior of the membrane is studied in order to obtain the profile of the membrane when submitted to a static differential pressure. In the second step, the dynamic behavior of the membrane is studied. Finally, the theoretical results obtained are compared with experiments in order to evaluate the accuracy of the model.

PACS no. 43.25.Lj, 43.38.-p, 43.75.Tv

1. Introduction

Acoustic transducers using curved clamped piezoelectric polymer films have been studied over the last few decades for different applications, such as earphones [1, 2], telephone transducers [3, 4] and [5], audio tweeters [6], ultrasonic sensors [7] or transducers for active noise control [8]. More recently, piezoelectric polymer films have been used to design air-borne parametric arrays.

A parametric array is a transducer which exploits a non linear interaction between two high frequency sound waves in order to generate a narrow beam of low frequency sound [9]. This kind of transducer has been studied extensively for underwater applications since the mid 60's [10, 11, 12, 13, 14, 15]. Applications in air propagation are more recent [16, 17]. Most parametric arrays specifically designed for air-borne applications consist of a set of piezolectric transducers made of piezoceramic, or making use of piezo-plastic membrane [18, 19]. In the latter, the parametric array is classically formed by a set of dome-shaped elementary transducers. The dome-shape is obtained by means of a static differential pressure held between the two faces of a clamped circular membrane. In order to properly design such a parametric array, a precise modeling of each elementary transducer is required.

Theoretical models of the behaviour of curved clamped piezoelectric polymer films are already available in literature [1, 4, 5]. However, these analytical models usually assume drastic approximations. Some of them [1, 4] assume quasi-static approximation which would imply evaluating *a posteriori* the inertial factor in order to describe approximately the behavior of the system around its first resonance frequency. Others assume *in vacuo* approximation [5] which does not take into account the effect of the acoustic load on the behavior of the system.

Therefore, the aim of the study presented here is to develop an analytical model avoiding these approximations. This model aims at precisely describing the behavior of a dome-shaped piezoelectric elementary transducer over a large frequency range, including explicitly the effect of the acoustic load.

In this paper, the theoretical description of the transducer's behavior is conducted in two steps. In the first step, the static behavior of the membrane is studied in order to obtained the profile of the membrane when submitted to a static differential pressure between its two faces. From this static study, the mechanical parameters used for the dynamical study can be estimated. In the second step, the dynamical behavior of the membrane is studied. In particular, the efficiency is derived. Finally, the theoretical results obtained are compared with experiments in order to evaluate the accuracy of the model.

Received 24 August 2010,
accepted 22 June 2011.

2. Dome-shaped transducer under study

The transducer under study is schematically depicted in Figure 1. It is a dome-shaped loudspeaker made of a PVDF bioriented film metallised on each side. The film is characterized by its thickness h_m, its Young modulus E_m, its Poisson's ratio ν_m, its density ρ_m and the piezoelectric coefficient d_3 assumed to be identical for both principal longitudinal directions ($d_3 = d_{3,1} = d_{3,2}$). The back side of the membrane is coupled with a rear cylindrical cavity of

© S. Hirzel Verlag · EAA

Document downloaded by @DAEL, 2026-11-08 06:32:04 - personal use only

radius a and depth l_c. The loudspeaker is mounted on an infinite screen. The front side of the membrane radiates in a half space. The membrane is initially a flat circular membrane of radius a clamped at its periphery. The dome shape described by static displacement w_s (positive for negative z) is obtained by means of a static differential pressure $P = P_0 - P_{cav}$ held between the two faces of the membrane, with P_0 the atmospheric static pressure and P_{cav} the actual static pressure in the rear cavity. In practice, the static pressure inside the cavity is lower than the atmospheric pressure, maintained by using a vacuum pump connected to the rear cavity. When supplying an oscillating electric voltage U between its two faces, the piezoelectric membrane experiences an oscillating mechanical strain responsible for its radial elongation. With the membrane being clamped at its periphery, the radial elongation turns into a oscillating transverse displacement w_d (positive for positive z) leading to an acoustic radiation.

3. Analytical description of the transducer behavior

As mentioned in the introduction, the analytical description of the transducer behavior is conducted in two steps. Firstly, a classical model for the static deflection of the membrane is presented in section 3.1. Then, a new model describing the dynamical response of the membrane submitted to an oscillating voltage is presented in section 3.2.

3.1. Static profile of the membrane

In this paper, the study of the static displacement of a circular membrane under static differential pressure is based on the description given by Abram [1]. In this description, the simplifying approximation of a spherical dome shape is considered, with the central displacement of the film $w_s(0)$ assumed to be small compared to the radius a of the initially flat circular membrane ($w_s(0)/a \ll 1$). This approximation allows one to express the strain S in the film and the mechanical tension T_m as a function of the central displacement of the film

$$S = \frac{w_s(0)^2}{2a^2} + C, \tag{1}$$

and

$$T_m = \frac{Pa^2}{4w_s(0)}, \tag{2}$$

where the coefficient C takes into account the condition of the diaphragm before applying static differential pressure. In the case of a perfect diaphragm (no slackness or tension), the coefficient C is equal to zero. Then, writing the mechanical equilibrium equation

$$S = \frac{1 - \nu_m}{h_m E_m} T_m, \tag{3}$$

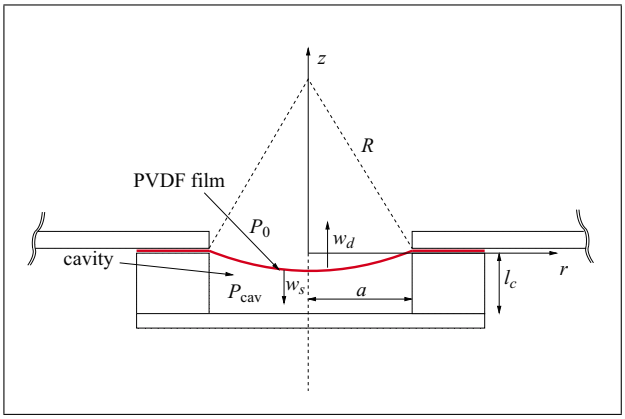


Figure 1. Schematic cross sectional view of the PVDF transducer mounted in a infinite screen.

allows one to derive the following expression for the central displacement of the membrane,

$$w_s(0) = a\sqrt[3]{\frac{Pa}{2E_m h}(1 - \nu_m)}. \tag{4}$$

As the membrane displacement is assumed to be a spherical dome, the radius of curvature R is written

$$R = \frac{w_s(0)^2 + a^2}{2w_s(0)}. \tag{5}$$

For small maximum displacement $w_s(0)$ compared with the film radius a,$w_s(0)/a \ll 1$, this expression can be simplified as

$$R = \frac{a^2}{2w_s(0)}. \tag{6}$$

Then, using this simplified expression in equation (2), the following simplified expression for the tension at rest T_m is obtained [5],

$$T_m = \frac{RP}{2}. \tag{7}$$

Assuming a large radius of curvature R compared with the radius a leads to the following simplified expression for the static radial profile of the dome-shaped membrane

$$w_s(r) = w_s(0)\left[1 - \left(\frac{r}{a}\right)^2\right]. \tag{8}$$

3.2. Dynamic behavior of the membrane

3.2.1. Literature review

The dynamic behaviour of a dome shape loudspeaker has already been studied by Davies *et al.*[4] and Garner *et al.* [5].

Davies considers that both faces of the PVDF loudspeaker radiate into a closed cavity, such as an earphone. He assumes that the membrane inertia effects are neglected and estimates the loudspeaker sensitivity in the cavity at low frequency (below the membrane resonance). This

Document downloaded by @DAEL, 2026-11-08 06:32:04 - personal use only

model cannot be applied to the device under study in this paper, firstly because the inertia effects of the membrane have to be taken into account in order to describe the coupling with the cavity beyond the first membrane resonance frequency, and secondly, because the loudspeaker under study radiates in free space.

Garner considers a PVDF dome mounted on a compliant plastic foam on one side and radiating in a half free space thanks to a baffle on the other side. He shows that the membrane dynamic displacement $w_d(r)$ is the solution of the following equation,

$$r\left[1-\frac{1}{2}(\frac{r}{R})^2\right]\frac{\partial^2 w_d}{\partial r^2}+\left[1-\frac{3}{2}\left(\frac{r}{R}\right)^2\right]\frac{\partial w_d}{\partial r} +k_m^2 r\left[1+\frac{1}{2}\left(\frac{r}{R}\right)^2\right]w_d=\frac{r}{R}\frac{2d_3U}{T_m}\frac{E_m}{1-\nu_m}, \tag{9}$$

where

$$k_m^2=\omega^2\frac{\mu_m}{T_m}, \tag{10}$$

with μ_m the film surface density. Assuming the radius of curvature R much higher than the radius a, equation (9) becomes a Bessel's equation

$$\frac{\partial^2 w_d}{\partial r^2}+\frac{1}{r}\frac{\partial w_d}{\partial r}+k_m^2 w_d=\frac{2d_3U}{RT_m}\frac{E_m}{1-\nu_m}, \tag{11}$$

where the right hand term depends on both the film tension at rest T_m and the radius of curvature R. However, terms which take into account the coupling with the front and back acoustic loads are not written, leading to a model of a loudspeaker *in vacuo*. Therefore, this model cannot be applied to the device under study here.

Thus, an improved model, allowing the prediction of the dynamic displacement of the membrane w_d as a function of the electric voltage U, has to be developed. This model takes into account the coupling between the membrane and the front (radiation impedance) and rear (cavity impedance) acoustic loads.

3.2.2. Improved model

Equation of motion for the membrane The set of equations governing the velocity $v_d = j\omega w_d$ of the circular membrane clamped at its periphery is

$$\begin{cases} T_m(\Delta+k_m^2)v_d(r)=\mathrm{j}\omega\big(p_e(r,0)-p_i(r,0)+P_U\big), \\ v_d(a)=0, \end{cases} \tag{12}$$

where P_U is the equivalent pressure due to the electric voltage written as [5]

$$P_U=\frac{2Ud_3E_m}{R(1-\nu_m)}. \tag{13}$$

Equation (12) is derived directly from equation (11) for the dynamic displacement when taking into account the acoustic pressure p_i inside the rear cavity and the acoustic pressure p_e on the front side of the membrane.

Equation (12) can be simplified assuming that the pressure p_e results from the product of the radiation impedance Z_e and the membrane velocity, $p_e = Z_e v_d$, which enables to consider a modified wavenumber K given by [20]

$$K^2=k_m^2-\mathrm{j}\omega Z_e/T_m. \tag{14}$$

With this assumption, equation (12) becomes

$$\begin{cases} T_m(\Delta+K^2)v_d(r)=\mathrm{j}\omega\big(P_U-p_i(r,0)\big), \\ v_d(a)=0. \end{cases} \tag{15}$$

Assuming that there is no source inside the rear cavity, the acoustic pressure $p_i(r,0)$ on the rear side of the membrane ($z=0$) is given by the Green's formula,

$$p_i(r,0)=-\mathrm{j}\rho\omega\int\!\!\int_S G(r,0;r_0,0)v_d(r_0)\,\mathrm{d}S_0, \tag{16}$$

where ρ is the air density and where the Green's function $G(r,z;r_0,z_0)$ satisfies the following boundary conditions [21]

$$\partial_{n_0}G(\vec{r},\vec{r_0})=0, z=0, \tag{17}$$

$$\partial_{n_0}G(\vec{r},\vec{r_0})=0, z=-l_c, \tag{18}$$

$$\partial_{n_0}G(\vec{r},\vec{r_0})=0, r=a. \tag{19}$$

For any point in the cavity, this Green's function can be written [21]

$$G(r,z;r_0,z_0)=\sum_\nu -\frac{\cos\left(k_{z0\nu}(z-l_c)\right)}{k_{z0\nu}\sin\left(k_{z0\nu}l_c\right)}\frac{1}{\pi a^2 J_0^2(\gamma_{0\nu})} \cdot J_0(k_{w0\nu}r)J_0(k_{w0\nu}r_0), \tag{20}$$

where J_0 is the Bessel function of the first kind of order zero, where $k_{w0\nu}=\gamma_{0\nu}/a$, with $\gamma_{0\nu}$ the $(\nu+1)^{th}$ zero of first derivative of Bessel function J_0 and where $k_{z0\nu}$ is defined by $k_{z0\nu}^2=k_a^2-k_{w0\nu}^2$ (Appendix A1).

On the rear side of the membrane ($z=0$), it yields

$$G(r,0;r_0,0)=-\frac{1}{S_m}\sum_\nu\frac{J_0(k_{w0\nu}r)J_0(k_{w0\nu}r_0)}{k_{z0\nu}\tan\left(k_{z0\nu}l_c\right)J_0^2(\gamma_{0\nu})}, \tag{21}$$

where $S_m=\pi a^2$.

Finally, the equation governing the velocity of the membrane can be written

$$\begin{cases} T_m(\Delta+K^2)v_d(r) \\ +\rho\omega^2\int\!\!\int_S G(r,0;r_0,0)v_d(r_0)\,\mathrm{d}S_0=\mathrm{j}\omega P_U, \\ v_d(a)=0. \end{cases} \tag{22}$$

Solutions The solution of equation (22) is written as the sum of two terms,

$$v_d(r)=V_d\left[1-\frac{J_0(Kr)}{J_0(Ka)}\right] +\sum_{\nu\neq0}U_\nu\left[J_0(k_{w0\nu}r)-J_0(k_{w0\nu}a)\right], \tag{23}$$

in which V_d and U_ν are unknown coefficients. The first term on the right hand side of equation (23) represents the membrane velocity when taking into account the front radiation impedance [5] using the modified wavenumber K

Document downloaded by @DAEL, 2026-11-08 06:32:04 - personal use only

(see equation 14). The second term represents the effect of the back cavity.

Using equation (23) in equation (22) leads to (see more details in Appendix A1)

$$K^2 V_d + \sum_{v\neq 0} U_v \left[(K^2 - k_{w0v}^2) J_0(k_{w0v} r) - K^2 J_0(k_{w0v} a)\right] - \frac{\omega^2 \rho}{T_m} \frac{1}{k_{z00} \tan(k_{z00} l_c)} \left[V_d \left(1 - \frac{2J_1(Ka)}{KaJ_0(Ka)}\right) - \sum_{v'\neq 0} U_{v'} J_0(k_{w0v'} a)\right] - \frac{\omega^2 \rho}{T_m} \sum_{v\neq 0} \frac{J_0(k_{w0v} r)}{k_{z0v} \tan(k_{z0v} l_c)} \cdot \left[-\frac{2\pi V_d K a J_1(Ka)}{S_m (K^2 - k_{w0v}^2) J_0(Ka) J_0(k_{w0v} a)} + U_v\right] = \frac{\mathrm{j}\omega P_U}{T_m}. \quad (24)$$

Because this equation has to be verified for all r, equation (24) can be splitted into two equations,

$$K^2 V_d - \sum_{v\neq 0} U_v K^2 J_0(k_{w0v} a) = \frac{\mathrm{j}\omega P_U}{T_m} + \frac{\omega^2 \rho}{T_m k_{z00} \tan(k_{z00} l_c)} \left[V_d \left(1 - \frac{2J_1(Ka)}{KaJ_0(Ka)}\right) - \sum_{v'\neq 0} U_{v'} J_0(k_{w0v'} a)\right], \quad (25)$$

and

$$\sum_{v\neq 0} U_v (K^2 - k_{w0v}^2) J_0(k_{w0v} r) = \frac{\omega^2 \rho}{T_m} \sum_{v\neq 0} \frac{J_0(k_{w0v} r)}{k_{z0v} \tan(k_{z0v} L)} \left[U_v - \frac{2\pi V_d K a J_1(Ka)}{S_m (K^2 - k_{w0v}^2) J_0(Ka) J_0(k_{w0v} a)}\right]. \quad (26)$$

This set of two equations with the two unknowns V_d and U_v can easily be solved. Then, expression (23) of the membrane velocity can be written (Appendix A1)

$$v_d(r) = \frac{\mathrm{j}\omega P_U}{T_m} \frac{1 - \frac{J_0(Kr)}{J_0(Ka)} + \sum_{v\neq 0} \frac{\alpha_v}{\beta_v} (J_0(k_{w0v} r) - J_0(k_{w0v} a))}{K^2 - K_0^2 - \sum_{v\neq 0} \beta_0 \frac{\alpha_v}{\beta_v} J_0(k_{w0v} a)}, \quad (27)$$

where K_0 is given in Appendix A1 (equation A39).

The analytical expression of the pressure radiated by the PVDF loudspeaker is then given by the Rayleigh integral

$$p(z) = \mathrm{j}\omega\rho \iint_S v_d(r_0) G_R(z, r_0)\, \mathrm{d}S_0, \quad (28)$$

where $G_R(z, r_0) = \mathrm{e}^{-\mathrm{j}kd}/(2\pi d)$ with $d = \sqrt{z^2 + r_0^2}$. Due to revolution symmetry, the radiated pressure can finally be written

$$p(z) = \mathrm{j}\omega\rho \int_a v_d(r_0) \frac{\mathrm{e}^{-\mathrm{j}kd}}{d} r_0\, \mathrm{d}r_0. \quad (29)$$

Table I. PVDF transducer geometrical and physical parameters.

Parameter	Supplier value	Used value
Membrane radius a [cm]		4
Rear cavity length l_c [cm]		2
film thickness h_m [µm]		25
Young modulus E_m [GPa]	1–4	
Poisson's ratio ν_m	0.3–0.5	
Mechanical parameter $E_m/(1-\nu_m)$ [GPa]	1.43–8	5.9
Piezoelectric coeefficient d [pC/N]	3–5	5

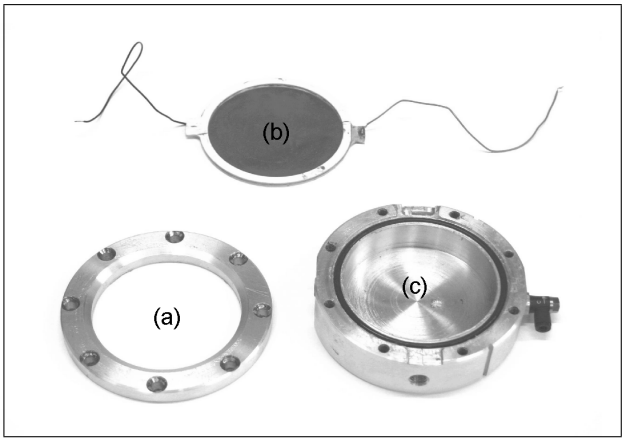


Figure 2. Experimental prototype. (a) ring clamping the membrane onto the back cavity. (b) PVDF membrane. (c) Back cavity.

4. Comparison with experiments

The experimental study presented in this section is conducted in two steps. Firstly, the static behaviour of the film is studied when submitted to a static pressure difference between its two faces. Then, the radiated acoustic pressure is measured and compared with theoretical predictions.

4.1. Experimental setup

The experimental prototype used for this study is shown in Figure 2. It is a loudspeaker made of a PVDF film clamped onto a back cavity with radius a and depth l_c. Through an opening in the cavity wall, a vacuum pump is used to maintain, inside the cavity, a static pressure lower than the atmospheric one. The numerical values of geometrical and physical parameters of this prototype are summarized in Table I.

4.2. Static measurements

Firstly, the static displacement w_s of the membrane is measured as a function of the radial coordinate r for a given static pressure difference P between the two faces of the membrane. The pressure difference is measured using a U-shaped tube filled with water. The membrane displacement is measured using a comparator. Experimental results are reported in Figure (3) for a static pressure difference

Document downloaded by @DAEL, 2026-11-08 06:32:04 - personal use only

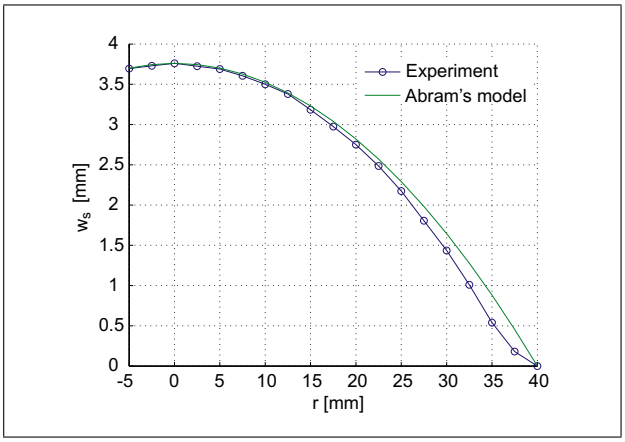


Figure 3. View of the static displacement $w_s(r)$ of a PVDF film. Comparison between measurement results and Abram's model for the two sets of parameters ($E_m = 1$ GPa, $\nu_m = 0.3$ and $E_m = 4$ GPa, $\nu_m = 0.5$). The membrane radius is 4 cm and the static pressure is 50 mbar.

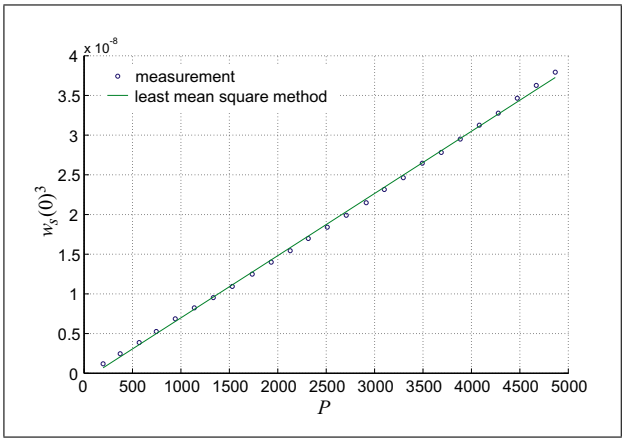


Figure 4. View of $w_s(0)^3$ as a function of static pressure P for a film with a thickness of 25 µm. The membrane radius is 4 cm and the maximum static pressure is 50 mbar.

$P = 50$ mb. The theoretical result obtained with Abram's model (Equation 3.1) for the same static displacement of the membrane centre $w_s(0)$ is also shown in Figure (3). Obviously, the experimental profile departs from a spherical one, especially near the boundary ($r = a$), where the derivative of the profile goes toward zero for the experimental case. Nevertheless, Abram's model is considered accurate enough to be used in this study. So, the radius of curvature R and the mechanical tension at rest T_m can be deduced from experimental static displacement $w_s(0)$, using equations (6) and (7) respectively.

In other respects, the film parameters are not known precisely and the supplier information shows a great variance (see table I). So, in order to estimate the numerical value of the mechanical parameter $\frac{E_m}{1-\nu_m}$, the static displacement of the membrane centre is measured for different static pressure differences p. As shown in Figure 4, the pressure P is proportional to $w_s(0)^3$, as predicted by equation 4. A least mean square minimization method is used in order to estimate the numerical value of parameter $\frac{E_m}{1-\nu_m}$ from experimental results. The value obtained with this method is given in Table I.

4.3. Radiated pressure measurements

Once the membrane is submitted to a static pressure diference, an electric voltage is supplied to the loudspeaker and the radiated pressure is measured.

The loudspeaker is mounted on a normalized IEC 268-5 baffle (1350 mm x 1650 mm) and placed in a full anechoic chamber. The electric voltage is supplied to the loudspeaker through a voltage amplifier TREK PZD350. The radiated pressure is measured using a microphone (Brüel & Kjær *4939*), located at 1 m in front of the loudspeaker on-axis.

Figures 5 and 6 show the radiated acoustic pressure measured at 1 m for an electric voltage of 1 V, for a static pressure difference $P = 50$ mb and $P = 100$ mb respectively. In the low frequency range, the measured pressure responses are high-pass filter, as expected for loudspeaker radiating in free space, with first resonance frequency around 1.8 kHz for 50 mbar and 2 kHz for 100 mbar. Beyond this first resonance frequency, the measured responses show marked antiresonances due to radial membrane modes.

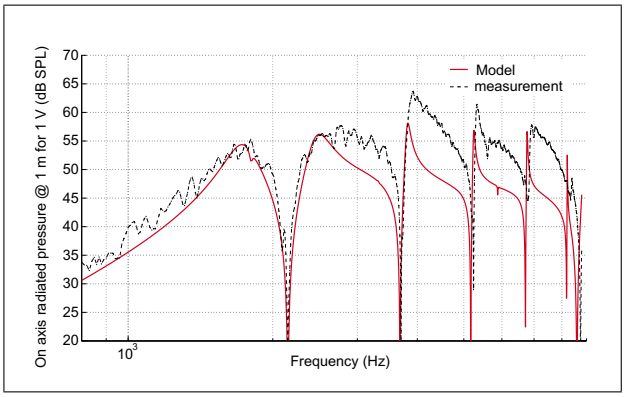


Figure 5. Radiated pressure for $P_0 = 50$ mb. Comparison between measurement and analytical model using the parameters given in Table I.

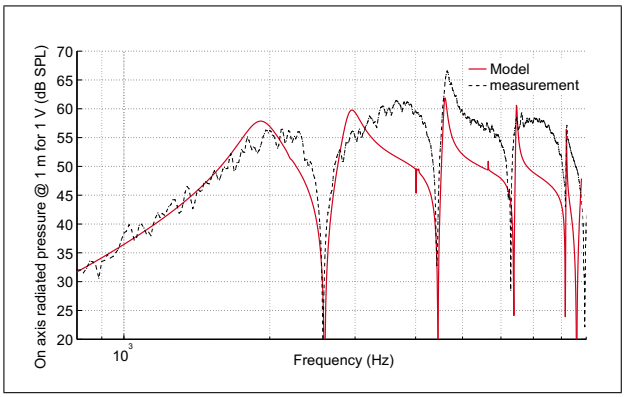


Figure 6. Radiated pressure for $P_0 = 100$ mb. Comparison between measurement and analytical model using the parameters given in Table I.

Document downloaded by @DAEL, 2026-11-08 06:32:04 - personal use only

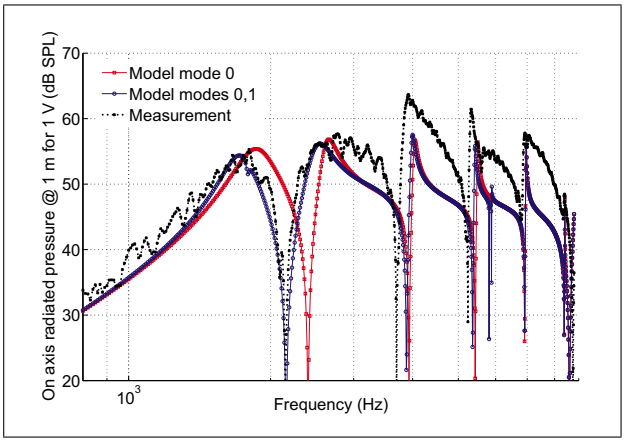


Figure 7. Effect of the number of modes on the predicted acoustic response of the PVDF loudspeaker.

The theoretical radiated pressure is also shown on these figures. The radiated pressure is calculated thanks to the Rayleigh integral (equation 29), where the membrane velocity is given by equation (27) taking into account 9 modes ($\nu = 0$ to 8). The membrane velocity is calculated assuming that the radiation impedance is $Z_e = \rho c$, where c is the speed of sound. This assumption seems to be reasonable since the relation $k_a a > 1$ (which corresponds roughly to $f > 1500\,\text{Hz}$, $k_a = 2\pi f/c$ being the wavenumber) is verified for the frequency range used for the experiment. The calculated pressure fits the measured one up to the first antiresonance. The model predicts relatively well the loudspeaker efficiency for low frequencies.

In order to understand the effect of the cavity on the loudspeaker response in the low frequency region, we present in Figure 7 a comparison between the experimental pressure response and the predicted response calculated when using 1 to 2 modes only ($\nu = 0$ to 1).

Figure 7 shows that mode 0 which represents the effect of the acoustic compliance of the back cavity, and mode 1 ($\gamma_{\mu\nu} = 3.83$) need to be taken into account at least in order to predict the acoustic response up to the first antiresonance.

When taking into account enough modes, the model obtains a good fit between the measured and calculated antiresonance frequencies for those greater than the first resonance frequency. Nevertheless, the model underestimates the high frequency efficiency (above first antiresonance).

5. Conclusion

A PVDF dome shaped loudspeaker has been studied, made of a PVDF membrane coupled with a back cavity in which a static pressure creates the dome shape.

An analytical model of the membrane movement has been developed taking into account the coupling with the air. This coupling is described at the front of the membrane using an equivalent radiation impedance. At the back of the membrane, the coupling with the back cavity is expressed using a Green's function based on cavity modes. This model assumes that the circumferential modes are neglected. It leads to an expression of the membrane velocity both as a function of the excitation voltage applied on the two faces of the membrane and as a function of the membrane and cavity parameters. The pressure radiated by the loudspeaker on-axis is expressed analytically as a function of the membrane velocity, assuming that the loudspeaker is mounted on an infinite baffle.

A prototype has been studied using static and dynamic measurements. Static measurements allow to deduce the mechanical parameters of the film by comparing the measured and calculated static displacement at the center of the membrane. Dynamic measurements performed in a full anechoic chamber using the loudspeaker mounted on a normalized IEC 268-5 baffle allow us to know the radiated acoustic pressure.

Comparisons between measured and calculated radiated pressure for two static pressures (50 mb and 100 mb) show good agreement for frequencies lower than the first antiresonance frequency of the radiated pressure. This antiresonance is due to the first radial mode of the membrane coupled with the cavity. Beyond the first antiresonance, the model can predict the higher antiresonance frequencies, but overestimates the efficiency of the loudspeaker.

For further work, it would be interesting to improve the model by taking into account the effect of circumferential modes in the membrane and cavity. Nevertheless, the analytical model given in this paper can be applied to predict the carrier frequency of a parametric array using dome shape PVDF loudspeakers assuming that the the carrier frequency equals the first resonance frequency of the loudspeaker.

Appendix

A1. Integral formulation for modeling the membrane-cavity coupling

This appendix presents the equations used for solving the problem presented in section 3.2.2 using the integral approach as proposed in [21].

A1.1. Membrane displacement

The expression of the membrane velocity v_d is given by

$$\triangle\, v_d(r) + K^2 v_d(r) = \frac{\mathrm{j}\omega}{T_m}\left(P_U - p_i(r,0)\right). \qquad \text{(A1)}$$

The acoustic pressure p_i inside the cavity is given by the Green's formulation

$$p_i(\vec{r}) = \iiint_D G(\vec{r},\vec{r}_0) f(\vec{r}_0)\,\mathrm{d}V + \iint_S \left[G(\vec{r},\vec{r}_0)\partial_{n_0} p(\vec{r}_0) - p(\vec{r}_0)\partial_{n_0} G(\vec{r},\vec{r}_0)\right]\mathrm{d}S_0. \qquad \text{(A2)}$$

Knowing there is no source inside the cavity, equation (A2) can be written

$$p_i(\vec{r}) = \iint_S G(\vec{r},\vec{r}_0)\partial_{n_0} p(\vec{r}_0)\,\mathrm{d}S_0, \qquad \text{(A3)}$$

Document downloaded by @DAEL, 2026-11-08 06:32:04 - personal use only

using a Green's function which satisfies boundary conditions

$$\partial_{n_0} G(\vec{r}, \vec{r_0}) = 0, \quad z = 0, \tag{A4}$$
$$\partial_{n_0} G(\vec{r}, \vec{r_0}) = 0, \quad z = -l_c, \tag{A5}$$
$$\partial_{n_0} G(\vec{r}, \vec{r_0}) = 0, \quad r = a. \tag{A6}$$

Knowing that

$$\partial_{n_0} p(\vec{r_0}) = -\mathrm{j} k_a \rho c v_d(\vec{r_0}), \tag{A7}$$

where ρ is the air density, c is the speed of sound in air, and $k_a = \omega/c$ is the wave number in air. The pressure acting on the rear side of the membrane inside the cavity is written for $\vec{r} = (r, \theta, z = 0)$

$$p_i(r, \theta, 0) = -\mathrm{j}\rho\omega \int\int_S G(r, \theta, 0; r_0, \theta_0, 0) v_d(r_0, \theta_0)\, \mathrm{d}S_0. \tag{A8}$$

Then, equation (A1) can be written

$$\triangle\, v_d(r, \theta) + K^2 v_d(r, \theta) + \frac{\omega^2 \rho}{T_m} \int\int_S G(r, \theta, 0; r_0, \theta_0, 0) v_d(r_0, \theta_0)\, \mathrm{d}S_0 = \frac{\mathrm{j}\omega}{T_m} P_U. \tag{A9}$$

A1.2. Cavity Green's function

The Green's function of the cylindrical cavity with radius a and length l_c is written as a the sum of the eigenfunctions of the cylinder [21]

$$G(r, \theta, z; r_0, \theta_0, z_0) = \sum_{\mu,\nu} \sum_{t=c,s} g_{\mu\nu}(z, z_0) \psi^t_{\mu\nu}(r_0, \theta_0) \psi^t_{\mu\nu}(r, \theta), \tag{A10}$$

where the eigenfunctions are for $t = c$ (for $cos\mu\theta$) and $t = s$ (for $sin\mu\theta$)

$$\psi^c_{\mu\nu}(r, \theta) = \frac{1}{a_\mu b_{\mu\nu}} \cos\mu\theta J_\mu(k_{w\mu\nu} r), \tag{A11}$$
$$\psi^s_{\mu\nu}(r, \theta) = \frac{1}{a_\mu b_{\mu\nu}} \sin\mu\theta J_\mu(k_{w\mu\nu} r). \tag{A12}$$

$k_{w\mu\nu}$ are the eigenvalues satisfying the boundary conditions

$$k_{w\mu\nu} = \frac{\gamma_{\mu\nu}}{a}, \tag{A13}$$

where $\gamma_{\mu\nu}$ represents the $(\nu+1)^{th}$ zero of the first derivative of the Bessel function J_μ. We assume in this work that only the first azimutal mode is considered ($\mu = 0$). Using this assumption, the eigenfunctions are written

$$\psi^c_{0\nu}(r, \theta) = \frac{1}{a_0 b_{0\nu}} J_0(k_{w0\nu} r), \tag{A14}$$
$$\psi^s_{0\nu}(r, \theta) = 0. \tag{A15}$$

The normalisation coefficients a_μ et $b_{\mu\nu}$ are given by (for $\mu = 0$)

$$a_0^2 = 2\pi \tag{A16}$$
$$b_{0\nu} = \frac{a^2}{2} J_0^2(\gamma_{0\nu}). \tag{A17}$$

Neglecting the viscothermal losses, coefficients $g_{\mu\nu}(z, z_0)$ are written for $z < z_0$ (with $z_0 = 0$)

$$g_{\mu\nu}(z, z_0) = -\frac{\cos\left(k_{z\mu\nu}(z - l_c)\right)}{k_{z\mu\nu} sin(k_{z\mu\nu} l_c)}, \tag{A18}$$

where

$$k^2_{z\mu\nu} = k_a^2 - k^2_{w\mu\nu}. \tag{A19}$$

The Green's function (equation A10) of the cavity can then be written, for $\mu = 0$,

$$G(r, z; r_0, z_0) = \sum_\nu -\frac{\cos\left(k_{z0\nu}(z - l_c)\right)}{k_{z0\nu} sin(k_{z0\nu} l_c)} \frac{1}{\pi a^2 J_0^2(\gamma_{0\nu})} J_0(k_{w0\nu} r) J_0(k_{w0\nu} r_0), \tag{A20}$$

and the Green's function used in the expression (A8) of the internal pressure acting on the rear side of the membrane is given by

$$G(r, 0; r_0, 0) = -\frac{1}{S_m} \sum_\nu \frac{J_0(k_{w0\nu} r) J_0(k_{w0\nu} r_0)}{k_{z0\nu} \tan\left(k_{z0\nu} l_c\right) J_0^2(\gamma_{0\nu})}, \tag{A21}$$

where $S_m = \pi a^2$.

A1.3. The Solution to the problem

The membrane velocity v_d is written as the sum of two terms. First term is given by Garner *et al.* [5] and corresponds to the membrane velocity *in vacuo*. Second term takes into account the coupling with the back cavity. The velocity is then written as

$$v_d(r) = V_d \left[1 - \frac{J_0(Kr)}{J_0(Ka)}\right] + \sum_{\nu \neq 0} U_\nu \left[J_0(k_{w0\nu} r) - J_0(k_{w0\nu} a)\right], \tag{A22}$$

where V_d and U_ν are two unknown coefficients that have to be determined.

Using the above expression of $v_d(r)$ in equation (A1) leads to the following expression,

$$K^2 V_d + \sum_{\nu \neq 0} U_\nu \left[(K^2 - k^2_{w0\nu}) J_0(k_{w0\nu} r) - K^2 J_0(k_{w0\nu} a)\right] = \frac{\mathrm{j}\omega}{T_m} \left(P_U - p_i(r, 0)\right). \tag{A23}$$

where

$$\frac{\mathrm{j}\omega}{T_m} p_i(r, 0) = \omega^2 \frac{\rho}{T_m} \int\int_S G(r, \theta, 0; r_0, \theta_0, 0) v_d(r_0, \theta_0)\, \mathrm{d}S_0, \tag{A24}$$

Document downloaded by @DAEL, 2026-11-08 06:32:04 - personal use only

leading to

$$\frac{\mathrm{j}\omega}{T_m} p_i(r,0) = -\frac{\omega^2\rho}{S_m T_m} \sum_{\nu} \frac{J_0(k_{w0\nu} r)}{k_{z0\nu} \tan(k_{z0\nu} l_c) J_0^2(\gamma_{0\nu})} \cdot \left[V_d - \sum_{\nu' \neq 0} U_{\nu'} J_0(k_{w0\nu'} a) \right] I_1(\nu) - \frac{\omega^2\rho}{S_m T_m} \sum_{\nu} \frac{J_0(k_{w0\nu} r)}{k_{z0\nu} \tan(k_{z0\nu} l_c) J_0^2(\gamma_{0\nu})} \cdot \left[-\frac{V_d}{J_0(Ka)} I_2(\nu) + \sum_{\nu' \neq 0} U_{\nu'} I_3(\nu,\nu') \right], \quad \text{(A25)}$$

with

$$I_1(\nu) = \int\int_S J_0(k_{w0\nu} r_0)\, \mathrm{d}S_0, \quad \text{(A26)}$$

$$I_2(\nu) = \int\int_S J_0(k_{w0\nu} r_0) J_0(K r_0)\, \mathrm{d}S_0, \quad \text{(A27)}$$

$$I_3(\nu,\nu') = \int\int_S J_0(k_{w0\nu} r_0) J_0(k_{w0\nu'} r_0)\, \mathrm{d}S_0. \quad \text{(A28)}$$

The integrals I_1, I_2 and I_3 are calculated as follows taking into account different cases

$$I_1(\nu) = \begin{cases} \pi a^2 & \text{if } \nu = 0, \\ \frac{a}{k_{w0\nu}} J_1(k_{w0\nu} a) = 0 & \text{if } \nu \neq 0, \end{cases} \quad \text{(A29)}$$

$$I_2(\nu) = \begin{cases} \frac{2\pi a}{K} J_1(Ka) & \text{if } \nu = 0, \\ \pi a^2 J_0^2(k_{w0\nu} a) & \text{if } \nu \neq 0 \text{ and } k_{w0\nu} = K, \\ \frac{K 2\pi a}{K^2 - k_{w0\nu}^2} J_1(Ka) J_0(k_{w0\nu} a) & \text{if } \nu \neq 0 \text{ and } k_{w0\nu} \neq K, \end{cases} \quad \text{(A30)}$$

$$I_3(\nu,\nu') = \begin{cases} 0 & \text{if } \nu = 0, \\ 0 & \text{if } \nu \neq \nu', \\ \pi a^2 J_0^2(k_{w0\nu} a) & \text{if } \nu = \nu'. \end{cases} \quad \text{(A31)}$$

Finally, equation (A23) can be written

$$K^2 V_d + \sum_{\nu \neq 0} U_\nu \left[(K^2 - k_{w0\nu}^2) J_0(k_{w0\nu} r) - K^2 J_0(k_{w0\nu} a) \right] = \frac{\mathrm{j}\omega}{T_m} P_U + \frac{\omega^2\rho}{T_m} \frac{1}{k_{z00} \tan(k_{z00} l_c)} \cdot \left[V_d \left(1 - \frac{2J_1(Ka)}{Ka J_0(Ka)} \right) - \sum_{\nu' \neq 0} U_{\nu'} J_0(k_{w0\nu'} a) \right] + \frac{\omega^2\rho}{T_m} \sum_{\nu \neq 0} \frac{J_0(k_{w0\nu} r)}{k_{z0\nu} \tan(k_{z0\nu} l_c)} \cdot \left[-\frac{2\pi V_d K a J_1(Ka)}{S_m (K^2 - k_{w0\nu}^2) J_0(Ka) J_0(k_{w0\nu} a)} + U_\nu \right]. \quad \text{(A32)}$$

Because this equation has to be verified for all r, equation (A32) can be split into the following two equations,

$$K^2 V_d - \sum_{\nu \neq 0} U_\nu k_m^2 J_0(k_{w0\nu} a) = \frac{\mathrm{j}\omega P_U}{T_m} + \frac{\omega^2\rho}{T_m k_{z00} \tan(k_{z00} l_c)} \cdot \left[V_d \left(1 - \frac{2J_1(Ka)}{Ka J_0(Ka)} \right) - \sum_{\nu' \neq 0} U_{\nu'} J_0(k_{w0\nu'} a) \right], \quad \text{(A33)}$$

and

$$\sum_{\nu \neq 0} U_\nu (k_m^2 - k_{w0\nu}^2) J_0(k_{w0\nu} r) = \frac{\omega^2\rho}{T_m} \sum_{\nu \neq 0} \frac{J_0(k_{w0\nu} r)}{k_{z0\nu} \tan(k_{z0\nu} L)} \cdot \left[U_\nu - \frac{2\pi V_d K a J_1(Ka)}{S_m (K^2 - k_{w0\nu}^2) J_0(Ka) J_0(k_{w0\nu} a)} \right]. \quad \text{(A34)}$$

Using the notation

$$\alpha_\nu = \frac{2\omega^2\rho K J_1(Ka)}{a T_m k_{z0\nu} \tan(k_{z0\nu} l_c)(K^2 - k_{w0\nu}^2) J_0(Ka) J_0(k_{w0\nu} a)}, \quad \text{(A35)}$$

and

$$\beta_\nu = K^2 - k_{w0\nu}^2 - \frac{\omega^2\rho}{T_m k_{z0\nu} \tan(k_{z0\nu} l_c)}, \quad \text{(A36)}$$

equation (A35) leads to

$$U_\nu = \frac{\alpha_\nu}{\beta_\nu} V_d. \quad \text{(A37)}$$

Equation (A34) can be written

$$V_d (K^2 - K_0^2) = \frac{\mathrm{j}\omega P_U}{T_m} + \sum_{\nu \neq 0} \frac{\alpha_\nu}{\beta_\nu} V_d J_0(k_{w0\nu} a) \beta_0, \quad \text{(A38)}$$

with

$$K_0^2 = \frac{\omega^2\rho}{T_m k_{z00} \tan(k_{z00} l_c)} \left(1 - \frac{2J_1(Ka)}{Ka J_0(Ka)} \right). \quad \text{(A39)}$$

By using relations (A37) and (A38) in equation (27) that gives $v_d(r)$, the membrane velocity can be written

$$v_d(r) = \frac{\mathrm{j}\omega P_U}{T_m} \frac{1 - \frac{J_0(Kr)}{J_0(Ka)} + \sum_{\nu \neq 0} \frac{\alpha_\nu}{\beta_\nu} (J_0(k_{w0\nu} r) - J_0(k_{w0\nu} a))}{K^2 - K_0^2 - \sum_{\nu \neq 0} \beta_0 \frac{\alpha_\nu}{\beta_\nu} J_0(k_{w0\nu} a)}. \quad \text{(A40)}$$

Acknowledgments

Many thanks to James Blondeau, Hervé Mézière from LAUM and Kevin Meder and Jean Paul Schmitt from ISL for their help in the mechanical and experimental work. Many thanks to Marilyn Twell for the corrections of the English text.

Document downloaded by @DAEL, 2026-11-08 06:32:04 - personal use only

References

[1] R. Abram: The theory of a piezoelectric plastic film transducer for earphones. Journal of Physics D Applied Physics **13** (1980) 201–207.

[2] M. Tamura, T. Yamaguchi, T. Oyaba, T. Yoshimi: Electroacoustic transducers with piezoelectric high polymer films. Journal of the Audio Engineering Society **23** (1975) 21–26.

[3] W. Cragg, N. Tester: Telephone transducers using piezoelectric polymer foil. Electr. Commun. **52** (1977) 312–314.

[4] G. Davies, P. Murphy, G. Maurer: A theoretical and experimental study of a model piezoelectric membrane headphone. The Journal of the Acoustical Society of America **76** (1984) 661.

[5] G. Garner, A. Holden: Tone ringer using polyvinylidene fluoride (PVDF) piezoelectric film. The Journal of the Acoustical Society of America **83** (1988) 1940.

[6] P. Ueberschlag: Pvdf piezoelectric polymer. Sensor Review **21** (2001) 118 – 126.

[7] A. Fiorillo: Noise analysis in air-coupled pvdf ultrasonic sensors. IEEE Transactions on Ultrasonics, Ferroelectrics, and Frequency Control **47** (november 2000) 1432–1437.

[8] P. Lotton, M. Bruneau, Z. Skvor, A.-M. Bruneau: A model to describe the behaviour of a laterally radiating piezoelectric loudspeaker. Applied Acoustics **58** (december 1999) 419–442.

[9] P. Westerwelt: Parametric acoustic array. The Journal of the Acoustical Society of America **35** (1963) 535–537.

[10] H. Berktay: Possible exploitation of nonlinear acoustics in underwater transmitting applications. Journal of Sound and Vibration **2** (1965) 435–461.

[11] T. Muir, J. Blue: Experiments on the acoustic modulation of large amplitude waves. The Journal of the Acoustical Society of America **46** (1969) 227–232.

[12] T. Muir, J. Willette: Parametric acoustic transmitting arrays,. The Journal of the Acoustical Society of America **52** (1972) 1481–1486.

[13] H. Berktay, D. Leahy: Farfield performance of parametric transmitters. The Journal of the Acoustical Society of America **55** (1974) 539–546.

[14] F. Fenlon: On the performance of a dual frequency parametric source via matched asymptotic solutions of burgers' equation. The Journal of the Acoustical Society of America **55** (1974) 34–36.

[15] C. Darvennes, M. Hamilton, J. Tjotta, S. Tjotta: Effects of absorption on the nonlinear interaction of sound beams. The Journal of the Acoustical Society of America **89** (1991) 1028–1036.

[16] M. Bennett, D. Blackstock: Parametric array in air. The Journal of the Acoustical Society of America **57** (1975) 562–568.

[17] S. Trenchard, A. Coppens: Experimental study of a saturated parametric array in air. The Journal of the Acoustical Society of America **68** (1980) 1214–1216.

[18] X. Limei, C. Jianfang, H. Dagui: Design and characterization of a PVDF ultrasonic acoustic transducer applied in audio beam loudspeaker. Mechatronics and Automation, 2005 IEEE International Conference, 2005, 1992– 1997.

[19] J. Yang, W.-S. Gana, K.-S. Tan, M.-H. Er: Acoustic beamforming of a parametric speaker comprising ultrasonic transducers. Sensors and Actuators A **125** (october 2005) 91–99.

[20] B. Lihoreau, P. Lotton, M. Bruneau, V. Gusev: Piezoelectric Source Exciting Thermoacoustic Resonator: Analytical Modelling and Experiment. Acta Acustica united with Acustica **88** (2002) 986–997.

[21] C. Guianvarc h, J. Durocher, M. Bruneau, A. Bruneau: Improved formulation of the acoustic transfer admittance of cylindrical cavities. Acta Acustica united with Acustica **92** (2006) 345.

Document downloaded by @DAEL, 2026-11-08 06:32:04 - personal use only